Challenge Journal of Concrete Research Letters

Research Article

Determining datum temperature and apparent activation energy: an approach for mineral admixtures incorporated cementitious systems

Muhammet Atasever [a,*], Mustafa Tokyay [b]

[a] Department of Civil Engineering, Abdullah Gül University, 38080 Kayseri, Türkiye
[b] Department of Civil Engineering, Middle East Technical University, 06800 Ankara, Türkiye

ABSTRACT

The maturity method is used to predict the strength of concrete by monitoring its temperature history. Accuracy of maturity method relies on the dependable determination of the datum temperature and the apparent activation energy. The current study introduces a new approach, complementing those in ASTM C1074-11, for determining the datum temperature and apparent activation energy. The experimental study involved using two different mineral additives to portland cement at 6%, 20%, and 35% replacement amounts. The mortars were then cured at temperatures of 5, 20, and 40 °C, and their strengths were determined. Subsequently, the datum temperatures and apparent activation energies for these mixtures were calculated using both the proposed approach and the alternatives from ASTM C1074-11. Strength estimations were conducted in conjunction with commonly used maturity functions. The results indicate that the proposed approach determines the datum temperature and apparent activation energy reliably for mineral admixture-incorporated mortars. Furthermore, the predicted strengths, derived from the datum temperature and apparent activation energy calculated through the proposed approach, show a closer alignment with the experimental results when applying the Nurse-Saul and Hansen-Pedersen equations, as opposed to the Rastrup and Weaver-Sadgrove models.

ARTICLE INFO

Article history:
Received 12 July 2024
Revised 31 August 2024
Accepted 12 September 2024

Keywords:
Maturity method
Datum temperature
Apparent activation energy
Mineral admixture

1. Introduction

The maturity method is a technique that is used for estimating the strength of concrete by taking temperature and time into account. Accuracy of the method relies primarily on dependable determination of the datum temperature and apparent activation energy. Maturity of concrete is generally expressed in terms of a temperature-time relationship and its equivalent age. The most well-known function for the temperature-time relationship is the Nurse-Saul equation, as given in Eq. (1).

$$M = \sum_0^t (T - T_0) \cdot \Delta t \quad (1)$$

where M (degree-days or degree-hours) is maturity index at age t, T (°C) is the average concrete temperature during the time interval, Δt, T_0 (°C) is datum temperature and Δt (days or hours) is time interval.

The principal idea of Eq. (1) is that concretes of the same mix and maturity tend to exhibit same strength. However, due to its linear character, Nurse-Saul equation often fails to provide accurate strength estimates outside the temperature range of 0-40 °C (Miller et al. 2022; Soutsos et al. 2018, 2021). To address this limitation, several alternative equations have been proposed, including those by Rastrup (Rastrup 1954), Weaver and Sadgrove (Weaver and Sadgrove 1971), Hansen and Pedersen (Hansen and Pedersen 1977). These equations are given as Eq. (2) to Eq. (4), respectively.

$$t_e = \sum_0^t 2^{(T-T_r)/10} \cdot \Delta t \quad (2)$$

$$t_e = \sum_0^t \left(\frac{T+16}{T_r+16}\right)^2 \cdot \Delta t \quad (3)$$

$$t_e = \sum_0^t e^{\frac{-E_a}{R}\left(\frac{1}{T+273} - \frac{1}{T_r+273}\right)} \cdot \Delta t \quad (4)$$

* *Corresponding author*. Tel.: +90-352-224-8800 ; E-mail address: muhammet.atasever@agu.edu.tr (M. Atasever)
ISSN: 2548-0928 / DOI: https://doi.org/10.20528/cjcrl.2024.04.004

for $T \geq 20$ °C E_a=33500 J/mol
for $T < 20$ °C E_a=33500+1470 (20-T) J/mol

where t_e (days or hours) is equivalent age, E_a (J/mol) is apparent activation energy, R (8.314 J/mol-°K) is gas constant, T (°C) is the average concrete temperature during the time interval, Δt, T_r (°C) is reference temperature, Δt (days or hours) is time interval.

Among these four equations, the Nurse-Saul equation (Eq. (1)) requires a datum temperature, whereas the Hansen-Pedersen equation (Eq. (4)) necessitates an apparent activation energy. The datum temperature in here refers to the minimum temperature at which concrete begins to gain strength (Nixon et al. 2008) and the apparent activation energy is defined as the smallest amount of energy required for concrete to start gaining strength (Shukla and Mishra 2015). ASTM C1074-11 (2011) suggests that the datum temperature can be set at 0 °C and the apparent activation energy of 41.5 kJ/mol is recommended for the concrete made without mineral admixtures. The standard also provides three alternatives to determine the datum temperature and apparent activation energy of concrete. The primary difference between them lies in the assumed starting point for strength development. According to ASTM C1074-11 (2011), Alternative I (A1.1.7) considers it to begin at the final setting time, while Alternative II (A1.1.8.1) assumes it starts after the final setting time during the hydration acceleration period, provided that the concrete has a reasonable ultimate strength. Alternative III (A1.1.8.2) assumes that strength development begins immediately after mixing (Atasever 2017). Among these alternatives, the second one that is given by Eq. (5) is generally being used for concretes without mineral admixtures:

$$S = S_u \cdot \frac{k_T \cdot (t - t_0)}{1 + k_T \cdot (t - t_0)} \tag{5}$$

where, S (MPa) is compressive strength at age t, S_u (MPa) is ultimate strength, k_T (1/days) is rate constant, t_0 (days) is age at start of strength development.

The theory gained acceptance due to its hyperbolic character and being more related with the hydration characteristics of portland cement. The method suggests strength development commences once concrete fully sets (Knudsen 1984). Various researchers have commented that Eq. (5) may not be as effective for blended cements containing mineral admixtures (Atasever 2017; Elçi and Yılmaz 2009; Ferraro et al. 2016; Soutsos et al. 2018). The revision in ASTM C1074-19 (2019) further reinforces this perspective. This viewpoint stems from the observations that the hydration mechanism and kinetics of blended cements vary considerably throughout the process. The differences are basically related with the type, amount, and characteristics of the mineral admixtures in the cement. Mineral admixtures affect the hydration process both physically and chemically. Physical effects are dilution, dispersion, alteration of particle size distribution, and nucleation. Dilution effect generally retards hydration whereas the other effects usually accelerate it. Chemically, their influence is seen in pozzolanic reactions, latent hydraulic reactions, and other related processes (Lam et al. 2023; Lothenbach et al. 2011; Moula et al. 2023; Wang et al. 2018). Another limitation of the function is its tendency to overestimate the long-term strengths of samples due to the negative impact of high curing temperatures (Miller et al. 2022; Soutsos et al. 2017, 2018, 2021). In this context, number of variables come into scene: the dissolution and stability of components within the pore fluid, a high concentration of hydroxyl ions, and the resulting chemical reaction rates. These factors collectively influence both the amount of hydration products and the early-age strength development in blended cements containing mineral admixtures (Zhang et al. 2021; Zuo et al. 2019). Additionally, the behavior of cementitious systems with incorporated mineral admixtures during the early-stages can be clarified using the "through-solution process". As highlighted by Tokyay (2016) and John and Lothenbach (2023), when the formation of hydration products primarily drives hydration, the water reaches saturation. This leads to uneven precipitation throughout its entire volume. Besides, in the later stages, adding mineral admixtures to portland cement leads to the formation of C-S-H gels through secondary hydration with portlandite. This process refines the pore structure and enhances the microstructure of the cementitious material. However, the distinct Ca/Si ratios in these cementitious systems cause differences in the interfacial transition zone (ITZ), affecting factors such as porosity, pore structure, and pore size. This variability also impacts the distribution of portland cement particles, which in turn influences the nucleation and precipitation of C-S-H gels (Dadsetan and Bai 2017; Liu et al. 2023; Lv et al. 2023).

This study describes a new methodology for determining the datum temperature and the apparent activation energy in cementitious systems with mineral admixtures. Employing a hyperbolic framework as explicated in Eq. (5), the proposed approach computes the ultimate strength and rate constant by considering early-age strength data recorded up to 14 days. This may seem as a contradiction for trass and blast furnace slag incorporated cementitious systems since pozzolanic and latent hydraulic reactions are generally far more gradual than hydration reactions. However, taking the early age data makes it possible to predict the time when a critical (sufficient) amount of calcium hydroxide is produced upon hydration of the portland cement and thus pozzolanic or latent hydraulic reactions start to contribute to the strength. So, Eq. (5) is rewritten as:

$$S = S_u \cdot \frac{k_T \cdot (t - t_{cr})}{1 + k_T \cdot (t - t_{cr})} \tag{6}$$

where, S (MPa) is compressive strength at age t, S_u (MPa) is ultimate strength, k_T (1/days) is rate constant, t_{cr} (days) is the age when the mineral admixture starts to contribute the strength.

The difference between Eqs. (5) and (6) lies in the use of t_{cr} instead of t_0. The calculation of t_{cr} involves two stages. In the first stage, the ultimate strength and rate constant are calculated. These two parameters, computed for each curing temperature, were derived using the test ages of 2, 7, and 14 days along with the corresponding strengths. However, a constraint was applied during the calculation of ultimate strength: the calculated ultimate strength must exceed the measured strength at 90 days. If not, the 90-day strength is taken as the ultimate strength. In the second stage, a strength-age graph is plotted for each curing temperature to determine t_{cr}, where a line is fitted. The age corresponding to half of the ultimate strength on this line is defined as the age when the mineral admixture starts to contribute to the strength. The datum temperatures and apparent activation energies for trass- and blast furnace slag-incorporated mortar mixes using the proposed approach and the methods given in ASTM C1074-11 (2011). Subsequently, the strength of these mixtures is evaluated via the Nurse-Saul, Rastrup, Weaver and Sadgrove, and Hansen and Pedersen equations. Comparative analysis is then conducted between the strength values derived from each equation.

2. Materials and Method

A portland cement (CEM I 42.5 R) was combined with two mineral admixtures: a volcanic tuff, trass (TRS) and a ground granulated blast furnace slag (BFS). These were used at replacement levels of 6%, 20%, and 35% by mass, with the specified levels determined in accordance with the guidelines outlined in TS EN 196-1 (2016). Standard sand was used in all mortar mixtures. Table 1 details the chemical and physical properties of the materials utilized in the study.

Table 1. Chemical and physical properties of the materials used.

Properties (%)	PC cement*	TRS	BFS
SiO_2	18.6	69.7	43.0
Al_2O_3	4.9	12.0	11.3
Fe_2O_3	2.5	1.7	0.9
CaO	61.6	2.8	33.0
MgO	2.3	0.9	6.2
SO_3	3.3	0.1	1.2
Na_2O	0.3	1.1	0.3
K_2O	0.8	1.8	0.7
TiO_2	-	0.3	0.6
LOI	5.1	7.3	0.3
Blaine fineness (m^2/kg)	340	540	470
Density (g/cm^3)	3.0	2.3	2.9

* The XRF result for PC cement was previously reported in the study of Atasever and Tokyay (2018).

The mixing, compaction, and moulding of mixtures were performed in accordance with TS EN 196-1 (2016), while maintaining a constant flow value (110±5%) as stipulated by ASTM C1437-20 (2020). All mortar samples were cast in moulds of 40×40×160 mm dimensions. Subsequently, the specimens were subjected to curing temperatures of 5, 20, and 40 °C until the designated test ages of 2, 7, 14, 28, and 90 days. The selection of test ages is based on the incorporation of mineral admixtures in the study. According to the proposed approach presented in Eq. (6), the ultimate strength must exceed the 90-day strength, consistent with the hydration mechanism of cementitious systems. The 2-day test was chosen based on the assumption that strength development in blends containing mineral admixtures does not begin before 2 days, as indicated in Eq. (6). On the other hand, the curing temperatures were chosen to encapsulate the spectrum of environmental conditions that concrete is likely to encounter across various regions of Türkiye, as documented in the study (Dombaycı 2009). Although regional temperature variations exist, the selected temperatures are representative of the thermal fluctuations experienced on a national scale, thereby facilitating a thorough evaluation of concrete performance under realistic and applicable conditions. The compressive strength obtained are the average of six specimens. The mixture proportions of the mortars are given in Table 2.

Table 2. Proportions of mortar mixtures (wt. %).

Mixture ID	PC cement	TRS	BFS	(w/b)
PC Control**	100	-	-	0.56
PC-TRS6	94	6	-	0.59
PC-TRS20	80	20	-	0.67
PC-TRS35	65	35	-	0.71
PC-BFS6	94	-	6	0.56
PC-BFS20	80	-	20	0.56
PC-BFS35	65	-	35	0.56

** The mix proportion for PC Control was previously employed in the study of Atasever and Tokyay (2018).

The normal consistency of pastes-having the same mixture proportions as specified in Table 2-was first determined according to ASTM C187-16 (2016). Subsequently, the final setting time of these mixtures was ascertained using ASTM C191-21 (2021). The results are presented in Fig. 1.

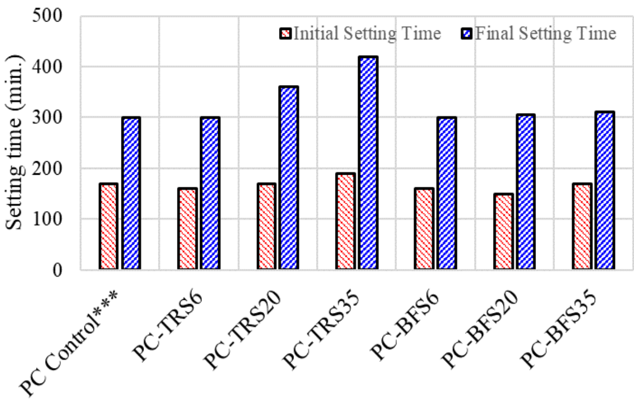

*** The setting time results for PC Control was previously reported in the study of Atasever and Tokyay (2018).

Fig. 1. Results of setting time of mixtures.

3. Results and Discussion

The strength development curves for all mixes cured at 5, 20 and 40 °C was plotted in Fig. 2 after 2, 7, 14, 28 and 90 days of curing.

The relationships between PC Control and the strength of mortar with mineral admixture over time (measured in days) show a striking similarity for the first 28 days. However, beyond 28 days, a notable difference emerges in the PC Control, PC-TRS20, and PC-BS6 mixtures. Mixtures cured at 20 °C displayed a reduced strength in comparison to those cured at 40 °C, indicating a temperature-dependent variation in the strength development of the mortar mixtures with mineral admixtures. This might be related to crossover effect, where high curing temperatures accelerate hydration and cause uneven distribution of hydration products, resulting in reduced porosity and higher early-age strength, but increased porosity and diminished strength at later ages (Escalante-García and Sharp 2001; Kim et al. 2002; Soutsos and Kanavaris 2020).

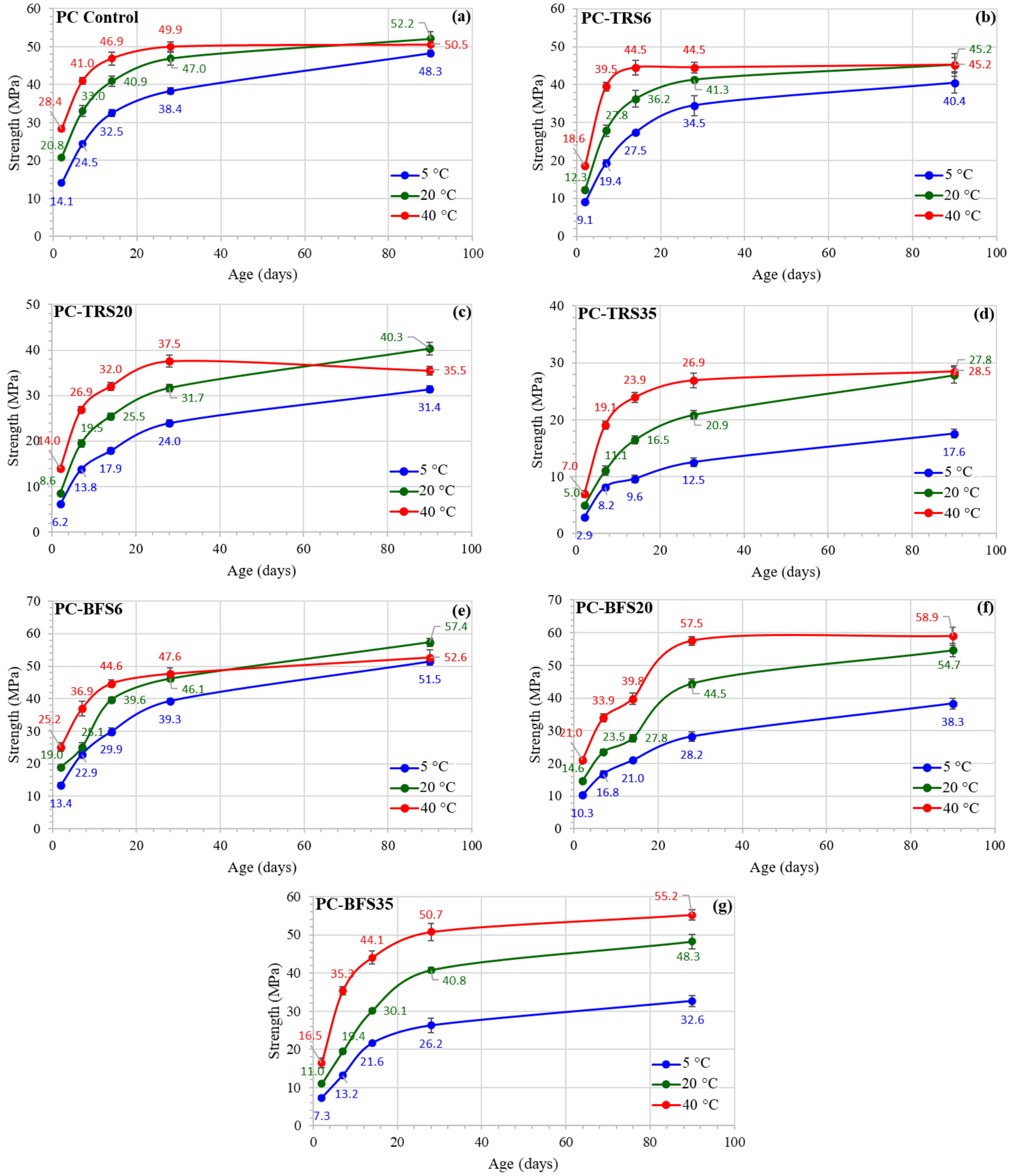

Fig. 2. Strength development curves at different curing temperature for:
(a) PC Control; (b) PC-TRS6; (c) PC-TRS20; (d) PC-TRS35; (e) PC-BFS6; (f) PC-BFS20; (g) PC-BFS35.

In low-heat concretes, strength development is slower, complicating late-age strength predictions. Adjusting the thermal curing parameters, such as heating rate, peak temperature, and curing duration, becomes crucial in addressing this challenge. Properly considering the crossover effect ensures accurate strength prediction and may necessitate modifications to the maturity equation to achieve precise forecasting of compressive strength (Klausen et al. 2018; Wang et al. 2023). Conversely, in the case of PC-TRS6 and PC-TRS35, the 90-day strengths exhibit minimal difference between samples cured at 20 and 40 °C. The observed consistency in 90-day strength at both 20 and 40 °C curing temperatures can be attributed to the eventual completion of hydration reactions that initially progress at a slower rate. This gradual completion may counterbalance the reduced speed of chemical reactions at room temperatures, leading to similar strengths across both temperature conditions.

3.1. Determining datum temperature and apparent activation energy: ASTM C1074-11 methods and the proposed approach

Three alternatives, detailed in ASTM C1074-11 (2011), along with proposed approach, were employed to determine apparent activation energy and datum temperature based on the strength data. Alternative 1 stands out among the three options in ASTM C1074-11 (2011), as it designates the final setting time as the age to begin strength development in cementitious materials. In contrast, other two alternatives predominantly utilize compressive strength results. Notably, Alternative 3 assumes that strength development in cementitious materials starts at the moment the cement-water reaction begins. Alternative 2, leveraging a hyperbolic equation, proves particularly pertinent for cements without mineral additives, unveiling a correlation absent in other variants. Therefore, a novel approach has been proposed, aiming to harmonize these discrepancies. This approach refines Eq. (5), ensuring that the ultimate strength reliably exceeds the 90-day benchmark. It further identifies the age to that the mineral admixture starts to contribute the strength by pozzolanic or latent hydraulic reactions. After completing the determination of rate constants and ultimate strengths by both ASTM C1074-11 (2011) procedures and the proposed approach, datum temperatures and apparent activation energies were computed, and results are given in Table 3. The activation energies, calculated from strengths, showed variations according to ASTM C1074-11 (2011) methods, ranging between 3.9 and 45.4 kJ/mol. In contrast, in the proposed approach, these values ranged from 20.5 to 33.8 kJ/mol. In the proposed approach, it was observed that as the amount of mineral additive increased, regardless of the type of mineral additive, the apparent activation energies of the blends increased compared to the PC Control. The only exception to this situation belongs to the PC-TRS6. Trass, which was 6 % by weight in this mixture, may have caused the dispersion of cement particles, allowing more space for the hydration of portland cement. This phenomenon has been observed in numerous studies involving the use of small quantities of mineral additives (Wang et al. 2024; Zhang et al. 2023; Jiang et al. 2023).

Table 3. Datum temperature and apparent activation energy of cementitious systems, calculated using different alternatives.

Mixture ID	Datum temperature (°C)			
	ASTM C1074-11 (2011)			Proposed approach
	Alternative 1	Alternative 2	Alternative 3	
PC Control****	-15.9	-7.0	1.6	-10.9
PC-TRS6	-26.6	-15.9	4.9	-9.2
PC-TRS20	-24.6	-7.5	4.1	-4.6
PC-TRS35	-104.9	-3.9	-0.5	1.2
PC-BFS6	-24.8	-6.9	-27.8	-9.0
PC-BFS20	-154.7	-10.2	-0.5	-9.6
PC-BFS35	-122.7	-1.4	-0.1	-7.2
	Apparent activation energy (kJ/mol)			
PC Control*****	19.3	24.7	37.9	22.5
PC-TRS6	14.4	21.2	45.3	20.5
PC-TRS20	15.2	34.2	39.7	29.6
PC-TRS35	5.8	34.2	31.0	33.8
PC-BFS6	15.8	26.6	15.5	22.7
PC-BFS20	3.9	23.6	26.1	23.6
PC-BFS35	5.0	26.9	32.7	25.3

**** The datum temperatures and apparent activation energies for PC Control, calculated according to the methods specified in ASTM C1074-11 (2011), were previously reported in the study of Atasever and Tokyay (2018).

The datum temperature for each mixture was determined through three different methods, as detailed in ASTM C1074-11 (2011) and the proposed approach. The differences in datum temperatures are primarily attributed to the differing approaches of each method in considering the time to begin strength development in the mixtures. In the case of the PC Control, datum temperatures exhibit relative consistency across these alternatives. Conversely, mixtures containing mineral additives show a tendency to produce illogical datum temperature results, especially with Alternative 1, as the amount of mineral additives increases. While the datum temperatures for each mixture, calculated using Alternatives 2 and 3, range from -27.8 to 4.9 °C, the range for the proposed approach varies between -11.2 and 1.2 °C. Although ASTM C1074-11 (2011) recommends a datum temperature of 0 °C for Type I cement without mineral admixtures, there is no universally applicable datum temperature for blends containing minerals as reported in the literature.

3.2. Assessment of the proposed approach

The maturities of the seven distinct mixtures were determined employing the equations given by Nurse-Saul (Eq. (1)), Rastrup (Eq. (2)), Weaver and Sadgrove (Eq. (3)), Hansen, and Pedersen (Eq. (4)). The datum temperature and apparent activation energy parameters utilized in these equations were derived by the proposed approach. Assuming a logarithmic relationship between the maturity index and strength for each equation, the compressive strengths at 2, 7, 14, 28, and 90 days for each mixture cured at 5, 20, and 40 °C were estimated. These theoretical values were then compared with the corresponding experimental results obtained. The comparative analysis is illustrated in Fig. 3.

In the context of these methodologies, the Nurse-Saul mandates the incorporation of datum temperature, whereas the Hansen-Pedersen is predicated upon the requisite of an apparent activation energy. In contrast, the Rastrup and Weaver-Sadgrove methods function exclusively based on the temperature history of the blends. Empirical analysis has demonstrated that, in terms of accuracy in strength predictions, the Nurse-Saul and Hansen-Pedersen equations outperform those of Rastrup and Weaver-Sadgrove, maintaining a margin of error confined to within 10 %. The observed discrepancy can be ascribed to the underlying assumptions of the Nurse-Saul equation, which asserts a linear correlation between strength development and temperature. Conversely, the Hansen-Pedersen function hypothesizes an exponential increase in strength gain rate with temperature (Soutsos et al. 2021). The linear model of the Nurse-Saul equation often results in an overestimation of the effects of lower early-age curing temperatures on the strength. In contrast, the exponential model of the Hansen-Pedersen function tends to underestimate the strength of blends in the early ages. Additionally, the Rastrup function proposes that the rate of reaction doubles with a 10 °C increment in reaction temperature, a principle that is paralleled in the Weaver-Sadgrove equation (Soutsos et al. 2018; Kanavaris et al. 2023). Nevertheless, such exponential strength gain rates are not commonly observed in trass and blast furnace slag incorporated blends, leading to deviations in strength estimates exceeding the 10 % margin of error.

4. Conclusions

This study investigated the determination of datum temperature and apparent activation energy values in trass and slag incorporated mortars, comparing traditional methods with a new approach. Furthermore, the datum temperatures and apparent activation energies determined through the proposed approach were employed in the maturity approaches of Nurse-Saul, Rastrup, Weaver-Sadgrove, and Hansen-Pedersen to estimate strength under various curing conditions and ages. Subsequently, these estimated strength values were compared with the experimental strength results. The following conclusions can be drawn:

- Excluding PC-TRS20, and PC-BFS6, the observed strength indicates a general trend where higher curing temperatures are associated with an increase in strength, while lower curing temperatures correspond to a decrease in strength.
- Datum temperature values, calculated using the proposed approach, range from -11 to 1 °C, while apparent activation energy values range between 20.5 kJ/mol and 33.8 kJ/mol. An observed trend indicates that as the mineral contribution increases in the cementitious system, the apparent activation energy value also increases.
- The strength estimation results, based on data temperatures and apparent activation energies derived through the proposed approach, indicated that the Nurse-Saul and Hansen-Pedersen equations provide predicted strengths much closer to the experimental results than the Rastrup and Weaver-Sadgrove models for the mineral admixture-incorporated mortars.
- The approach proposed in this investigation resulted in a reasonable determination of datum temperatures and apparent activation energies for trass- and slag-incorporated cement mortars.
- Similar research with other types of mineral admixtures would further refine the approach.

Acknowledgements
None declared.

Funding
The authors received no financial support for the research, authorship, and/or publication of this manuscript.

Conflict of Interest
The authors declared no potential conflicts of interest with respect to the research, authorship, and/or publication of this manuscript.

Author Contributions
All of the authors made substantial contributions to conception and design, or acquisition of data, or analysis and interpretation of data; were involved in drafting the manuscript or revising it critically for important intellectual content; and gave final approval of the version to be published.

Data Availability
The datasets created and/or analyzed during the current study are not publicly available, but are available from the corresponding author upon reasonable request.

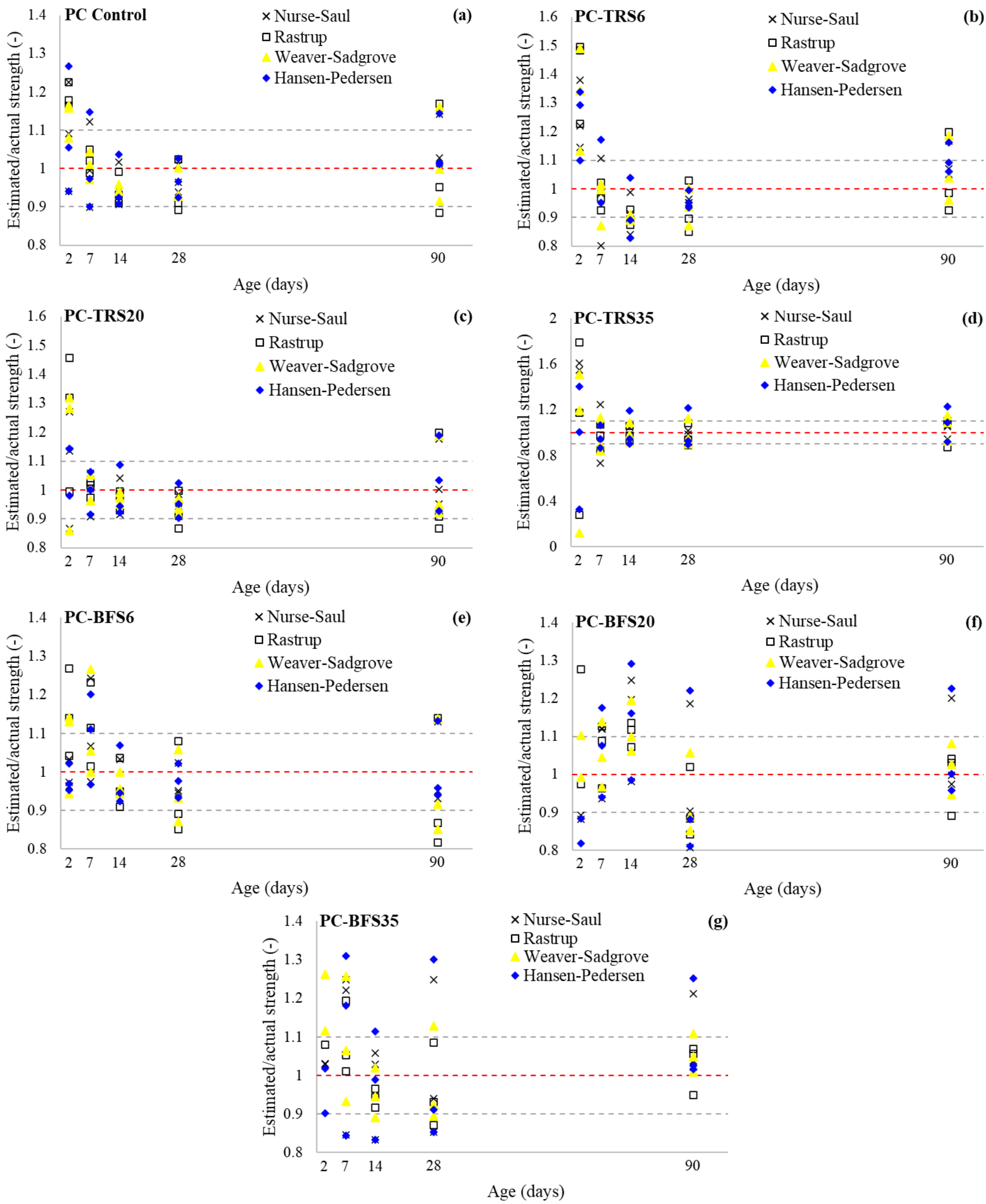

Fig. 3. Ratio of estimated/actual strengths for:
(a) PC Control; (b) PC-TRS6; (c) PC-TRS20; (d) PC-TRS35; (e) PC-BFS6; (f) PC-BFS20; (g) PC-BFS35.

References

ASTM C1074-11. (2011) Standard Practice for Estimating Concrete Strength by the Maturity Method. American Society for Testing and Materials, West Conshohocken, PA.

ASTM C1074-19. (2019) Standard Practice for Estimating Concrete Strength by the Maturity Method. American Society for Testing and Materials, West Conshohocken, PA.

ASTM C1437-20. (2020) Standard Test Method for Flow of Hydraulic Cement Mortar. American Society for Testing and Materials, West Conshohocken, PA.

ASTM C187-16. (2016) Standard Test Method for Amount of Water Required for Normal Consistency of Hydraulic
Cement Paste. American Society for Testing and Materials, West Conshohocken, PA.

ASTM C191-21. (2021) Standard Test Methods for Time of Setting of Hydraulic Cement by Vicat Needle. American Society for Testing and Materials, West Conshohocken, PA.

Atasever M (2017). Maturity and Equivalent Age Functions of Mineral Admixtures Incorporated Mortars. *M.Sc. thesis*, Middle East Technical University, Ankara, Türkiye.

Atasever M, Tokyay M (2018). Comparison of three alternatives for determining datum temperature and activation energy to estimate concrete strength by maturity method. *13th International Congress on Advances in Civil Engineering*, İzmir, Türkiye, 87-88.

Dadsetan S, Bai J (2017). Mechanical and microstructural properties of self-compacting concrete blended with metakaolin, ground granulated blast-furnace slag and fly ash. *Construction and Building Materials*, 146, 658–667.

Dombaycı ÖA (2009). Degree-days maps of Turkey for various base temperatures. *Energy*, 34(11), 1807-1812.

Elçi H, Yılmaz A (2009). Mineral katkılı çimentolarla üretilen betonun dayanımını tahmin etmede olgunluk yönteminin kullanılması. *Journal of the Faculty of Engineering and Architecture of Gazi University*, 24(3), 549–558. (in Turkish)

Escalante-García JI, Sharp JH (2001). The microstructure and mechanical properties of blended cements hydrated at various temperatures. *Cement and Concrete Research*, 31(5), 695–702.

Ferraro CC, Paris JM, Townsend TG, Tia M (2016). Evaluation of alternative pozzolanic materials for partial replacement of portland cement in concrete, Florida Department of Transportation Research Project, Gainesville, FL, USA. https://rosap.ntl.bts.gov/view/dot/31986 [accessed 09-05-2024].

Hansen PF, Pedersen EJ (1977). Maturity computer for controlled curing and hardening of concrete. *Nordisk Betong*, 21–25.

Jiang J, Wang, F, Wang L, Zhang J, Wang L (2023). Experimental investigation on effects of polyaniline-modified-lignin on cement-based materials: Strength, hydration and dispersion. *Construction and Building Materials*, 394, 131853.

John E, Lothenbach B (2023). Cement hydration mechanisms through time – a review. *Journal of Materials Science*, 58(24), 9805-9833.

Kanavaris F, Soutsos M, Chen JF (2023). Enabling sustainable rapid construction with high volume GGBS concrete through elevated temperature curing and maturity testing. *Journal of Building Engineering*, 63, 105434.

Kim JK, Han SH, Song YC (2002). Effect of temperature and aging on the mechanical properties of concrete: Part I. Experimental results. *Cement and Concrete Research,* 32, 1087-1094.

Klausen AE, Kanstad T, Bjøntegaard Ø, Sellevold EJ (2018). The effect of realistic curing temperature on the strength and E-modulus of concrete. *Materials and Structures,* 51(6), 168.

Knudsen T (1984). The dispersion model for hydration of portland cement I. General concepts. *Cement and Concrete Research*, 14(5), 622–630.

Lam A, Hamzaoui R, Kindinis A (2023). Structural and mechanical studies of a ground-granulated blast-furnace slag (GGBS) based binder and its use in earth concrete. *Materials Today: Proceedings*, in press.

Liu W, Zhu H, Wu X, Wan Y, Zheng W, Li H (2023). Comparative study on the performance of ultra-fine fly ash prepared by different techniques in Portland cement and alkali-activated material. *Construction and Building Materials*, 397, 132362.

Lothenbach B, Scrivener K, Hooton RD (2011). Supplementary cementitious materials. *Cement and Concrete Research*, 41(12), 1244–1256.

Lv X, Shi Y, Wang Y, Li J (2023). Utilization of phosphorus slag as fly ash replacement in low-heat Portland cement blends: Comparative study of hydration behaviors, physical properties, and life-cycle assessment. *Construction and Building Materials*, 396, 132346.

Miller D, Ho NM, Talebian N (2022). Monitoring of in-place strength in concrete structures using maturity method – An overview. *Structures*, 44, 1081–1104.

Moula S, Fraj AB, Wattez T, Bouasker M, Ali NBH (2023). Mechanical properties, carbon footprint and cost of ultra-high performance concrete containing ground granulated blast furnace slag. *Journal of Building Engineering*, 79, 107796.

Nixon JM, Schindler AK, Barnes RW, Wade SA (2008). Evaluation of the maturity method to estimate concrete strength in field applications, Research report no. 2. Alabama Department of Transportation, ALDOT research project 930-950. https://eng.auburn.edu/files/centers/hrc/930-590-2.pdf [accessed 09-05-2024].

Rastrup E (1954). Heat of hydration in concrete. *Magazine of Concrete Research,* 6(17), 79–92.

Shukla MK, Mishra SP (2015). In place strength of cement mortar/concrete using maturity and activation energy. *International Journal of Advanced Engineering Research and Studies*, 79–82.

Soutsos M, Hatzitheodorou A, Kanavaris F, Kwasny J (2017). Effect of temperature on the strength development of mortar mixes with GGBS and fly ash. *Magazine of Concrete Research*, 69(15), 787–801.

Soutsos M, Kanavaris F (2020). Compressive strength estimates for adiabatically cured concretes with the Modified Nurse-Saul (MNS) maturity function. *Construction and Building Materials*, 255, 119236.

Soutsos M, Kanavaris F, Elsageer M (2021). Accuracy of maturity functions' strength estimates for fly ash concretes cured at elevated temperatures. *Construction and Building Materials*, 266, 121043.

Soutsos M, Kanavaris F, Hatzitheodorou A (2018). Critical analysis of strength estimates from maturity functions. *Case Studies in Construction Materials*, 9, e00183.

Tokyay M (2016). Cement and Concrete Mineral Admixtures. 1st ed. CRC Press, Taylor and Francis Group, Florida, USA.

TS EN 196-1 (2016). Methods of testing cement-Part 1: Determination of strength. Turkish Standards Institute, TSE, Ankara, Türkiye.

Wang D, Shi C, Farzadnia N, Shi Z, Jia H, Ou Z (2018). A review on use of limestone powder in cement-based materials: Mechanism, hydration and microstructures. *Construction and Building Materials*, 181, 659–672.

Wang L, Wang J, Wang H, Qian X, Fang Y, Ge Y, Wang X, Zhao X, Amaral MLD (2024). Ascorbic acid: A green admixture for eco-efficient metakaolin blended cement with enhanced properties and corrosion resistance. *Cement and Concrete Composites*, 146, 105405.

Wang L, Zhou H, Zhang J, Wang Z, Zhang L, Nehdi ML (2023). Prediction of concrete strength considering thermal damage using a modified strength-maturity model. *Construction and Building Materials*, 400, 132779.

Weaver J, Sadgrove BM (1971). Striking Times of Formwork-Tables of Curing Periods to Achieve Given Strength. Construction Industry and Information Association, London, England.

Zhang J, Pan G, Yan Y (2021). Early hydration, mechanical strength and drying shrinkage of low-carbon alkali-activated Ti-extracted residues-fly ash cement and mortars. *Construction and Building Materials*, 293, 123517.

Zhang M, Li H, Na M, Zhou B, Zhang J (2023). Improving dispersion of recycled GFRP fiber in cement mortar with sodium hexametaphosphate. *Cement and Concrete Composites,* 143, 105232.

Zuo Y, Nedeljković M, Ye G (2019). Pore solution composition of alkali-activated slag/fly ash pastes. *Cement and Concrete Research,* 115, 230–250.